



Article

Cite this article: Brombacher A, Poole CR, Ezard THG, Wade BS (2024). Heterochrony in the evolution of the planktonic foraminifer *Globigerinoidesella fistulosa* from the *Trilobatus sacculifer* plexus. *Paleobiology* **50**, 582–591. <https://doi.org/10.1017/pab.2024.23>

Received: 19 May 2023
Revised: 21 July 2024
Accepted: 5 August 2024

Corresponding author:
Bridget S. Wade;
Email: b.wade@ucl.ac.uk

Heterochrony in the evolution of the planktonic foraminifer *Globigerinoidesella fistulosa* from the *Trilobatus sacculifer* plexus

Anieke Brombacher¹ , Christopher R. Poole² , Thomas H. G. Ezard³ and Bridget S. Wade²

¹School of Ocean and Earth Science, University of Southampton, Southampton SO14 3ZH, U.K.; present address: National Oceanography Centre, Southampton SO14 3ZH, U.K.

²Department of Earth Sciences, University College London, London WC1E 6BT, U.K.

³School of Ocean and Earth Science, University of Southampton, Southampton SO14 3ZH, U.K.

Non-technical Summary

Planktonic foraminifera are single-celled marine protists, roughly the size of a grain of sand. They have an extremely detailed fossil record: a teaspoonful of seafloor sediment contains more than 1000 fossil shells. Some species have unusually ornamental shapes, but it is not clear why or how these shapes evolved. Here, we study the developmental changes that led to the speciation of one particularly ornate species: *Globigerinoidesella fistulosa*. We find that changes in the developmental timing of adult life stages likely account for the complex morphology. This study highlights the complex morphological and developmental changes required to produce unusual shell shapes and highlights the importance of developmental changes in evolutionary origination.

Abstract

Planktonic foraminifera are extremely well suited to studying evolutionary change in the fossil record due to their abundant deposits and global distribution. Species are typically conservative in their shell morphology, with the same geometric shapes appearing repeatedly through iterative evolution, but the mechanisms behind the architectural limits on foraminiferal shell shape are still not well understood. To determine how these developmental constraints arise, we study morphological change leading up to the origination of the unusually ornate species *Globigerinoidesella fistulosa*. We measured the size and circularity of more than 900 specimens of *G. fistulosa*, its ancestor the *Trilobatus sacculifer* plexus, and intermediate forms from a site in the western equatorial Pacific. Our results show that the origination of *G. fistulosa* from the *T. sacculifer* plexus involved a combination of two heterochronic expressions: earlier onset of protuberances (pre-displacement) and a steeper allometric slope (acceleration) as compared with its ancestor. Our work provides a case study of the complex morphological and developmental changes required to produce unusual shell shapes and highlights the importance of developmental deviations in evolutionary origination.

Introduction

Trait variation among individuals provides the constituents for evolution through natural selection. Since the seminal works of Gould (1977) and Alberch et al. (1979), the importance of heterochrony in facilitating trait variation, and the resultant link between ontogeny and phylogeny, has become increasingly appreciated in the field of evolutionary developmental (paleo)biology (Keyte and Smith 2014; Dobrevá et al. 2022). Heterochrony may be broadly defined as a “change to the timing or rate of developmental events, relative to the same events in the ancestor” (McNamara 2012: p. 205; see comparable definitions in Gould [1977]; Alberch et al. [1979]; McNamara [1986]; McKinney and McNamara [1991]) and is widely regarded as having a central role in morphological evolution following the formalizations of Gould (1977) and Alberch et al. (1979).

There are two expressions of heterochrony, termed paedomorphosis and peramorphosis (Alberch et al. 1979; McNamara 1986). These are not processes, as is often erroneously assumed (see discussion in McNamara [1986]), but resultant expressions of trait morphology. Paedomorphosis results from a descendant morphospecies passing through fewer ontogenetic stages than its ancestor so that the descendant exhibits adult characters that were juvenile characters in the ancestor (Alberch et al. 1979; McNamara 1986). Conversely, peramorphosis results from the descendant passing through more ontogenetic stages than its ancestor, with the descendant exhibiting adult characters beyond that of the ancestor (Alberch et al. 1979; McNamara 1986).

© The Author(s), 2025. Published by Cambridge University Press on behalf of Paleontological Society. This is an Open Access article, distributed under the terms of the Creative Commons Attribution licence (<http://creativecommons.org/licenses/by/4.0/>), which permits unrestricted re-use, distribution and reproduction, provided the original article is properly cited.

PALEOBIOLOGY
A PUBLICATION OF THE
 PALEONTOLOGICAL SOCIETY

 **CAMBRIDGE**
UNIVERSITY PRESS



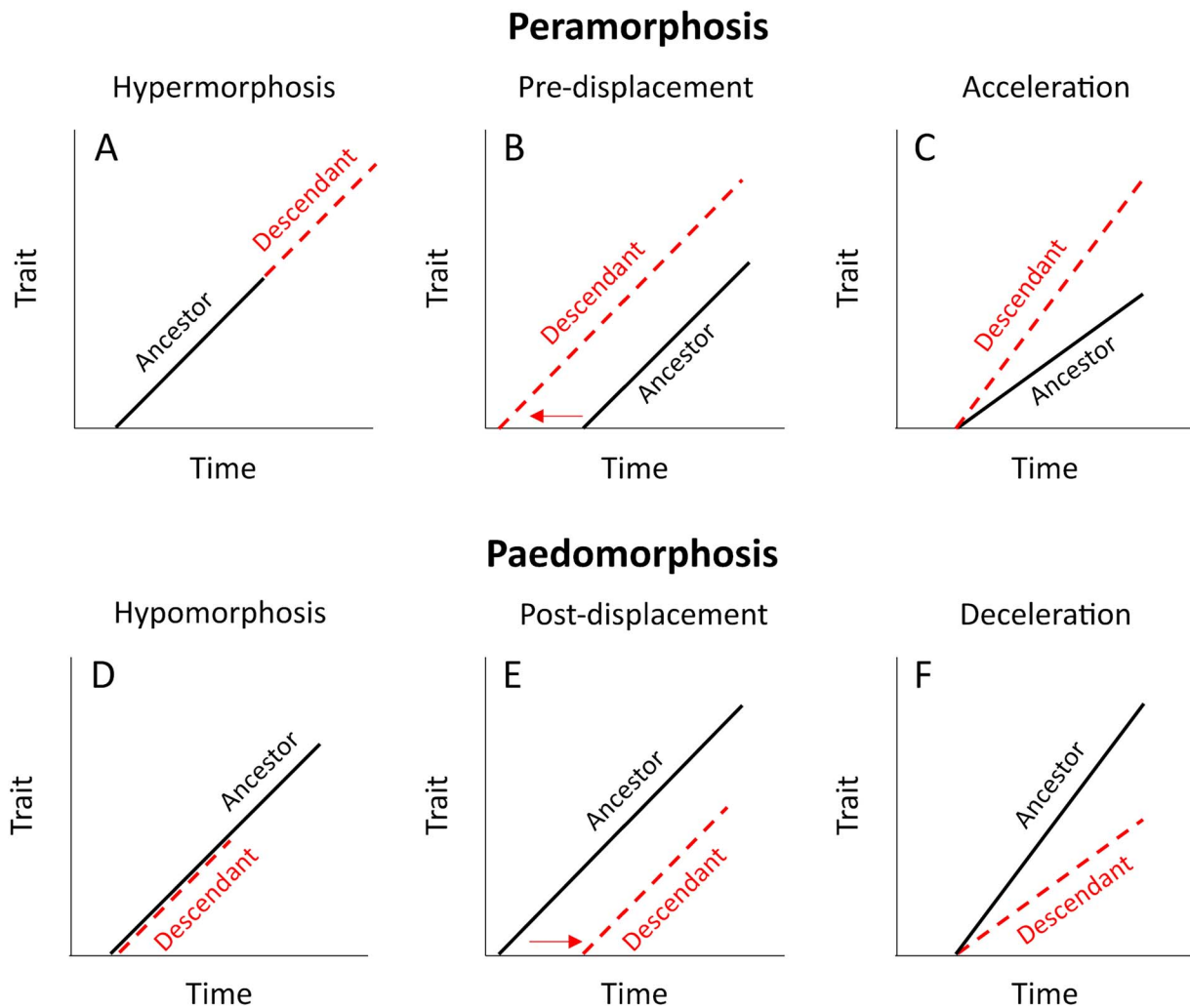


Figure 1. Schematic representations of trait development for the six types of heterochrony: **A**, hypermorphosis, wherein traits develop for longer in the descendant than the ancestor, while the rate and onset of trait development remain the same; **B**, pre-displacement, wherein the onset of descendant trait development starts earlier, while the rate of development remains the same; **C**, acceleration, wherein the rate of trait development is higher in the descendant species, while the onset of development is the same as the ancestor; **D**, hypomorphosis, wherein traits stop developing earlier in the descendant than the ancestor; **E**, post-displacement, wherein the onset of descendant trait development starts later than in the ancestor; and **F**, deceleration, wherein the rate of trait development is slower in the descendant than the ancestor.

Peramorphosis and paedomorphosis each result from three different (and opposing) heterochronic expressions. Peramorphosis includes hypermorphosis (continued development past the ancestor stage; Fig. 1A), pre-displacement (earlier onset of trait development in the descendant; Fig. 1B), and acceleration (faster development in the same amount of ontogenetic time as the ancestor; Fig. 1C). Paedomorphosis can result from hypomorphosis (reduced duration of development; Fig. 1D), post-displacement (later onset of trait development; Fig. 1E), or deceleration (slower trait development in the same amount of ontogenetic time as the ancestor; Fig. 1F). Note that following Reilly et al. (1997), two of the terms, hypomorphosis and deceleration, have been chosen to replace progenesis and neoteny of Alberch et al. (1979).

The fossil record is integral in studies assessing the role of heterochrony in the evolution of novel forms, as the traits of interest are often morphological. However, a long-acknowledged problem for paleontologists is determining the ontogenetic age of fossils. Although it is possible to infer age in some groups, such as fossil bivalves (Jones and Gould 1999), trilobites (Whittington 1957),

fish (Trueman et al. 2016), trees (Falcon-Lang 2015), and dinosaurs (Sander and Klein 2005; Sanchez et al. 2010), age is a poorly constrained parameter in most fossil organisms. To this end, size is often used as a proxy for age, and assessments of heterochrony are often identified under the framework of “allometric heterochrony” (McKinney 1986; McKinney and McNamara 1991; Wei 1994). Allometry describes trait covariation with body size according to a power relationship (Huxley 1932) and is therefore ideally suited to studies of heterochrony in the fossil record.

Planktonic foraminifera are a perfect target group for investigations into heterochrony. They have one of the best and most complete fossil records of any group (e.g., Norris 2000; Lazarus 2011), phylogenetic relationships between taxa are well resolved (Kennett and Srinivasan 1983; Olsson et al. 1999; Pearson et al. 2006a; Aze et al. 2011; Wade et al. 2018), and every chamber from the first (proloculus) to the last is retained through growth. Brummer et al. (1986, 1987) proposed five ontogenetic stages (prolocular, juvenile, neanic, adult, and terminal stages) in most morphospecies of planktonic foraminifera. Transitions from one

ontogenetic stage to the next are determined by a size threshold, rather than chamber number (Brummer et al. 1986, 1987; Wei et al. 1992; Schmidt et al. 2013; Caromel et al. 2016, 2017), so size is a good approximation for ontogenetic age in planktonic foraminifera. The concept of heterochrony could potentially explain the apparent lack of functional morphology in some foraminiferal traits. The evolution of traits without known functions could occur if a particular ontogenetic stage, rather than morphology, is selected for. Therefore, heterochrony presents an additional framework to study planktonic foraminifera evolution.

Here we investigate whether heterochrony took place during the origination of the planktonic foraminifer *Globigerinoidesella fistulosa*, a species characterized by an unusually ornate, digitate morphology with numerous protuberances on its final chamber(s) (Fig. 2). *G. fistulosa* evolved from the *Trilobatus sacculifer* plexus when a small subset of the *T. sacculifer* population (which includes morphospecies *Trilobatus trilobus*, *Trilobatus immaturus*, and *Trilobatus quadrilobatus*; see Poole and Wade [2019] for taxonomic discussion) increased in size, developed more extreme protuberances, and gradually diverged into *G. fistulosa* (Parker 1967; Chaisson and Leckie 1993; Poole and Wade 2019; Fig. 2). The complex shell shape of *G. fistulosa* stands out among planktonic foraminifera (see Chen et al. 2023), which are typically limited in morphological variation to the same basic shapes (Norris 1991). To understand the drivers of morphological innovation in foraminifera, we quantify test size and shape in *T. sacculifer* and *G. fistulosa* before and after the origination of *G. fistulosa*. We compare our results to previously published cases of heterochrony in planktonic foraminifera to assess whether developmental expressions can be rewired to overcome developmental constraints.

Materials and Methods

Study Species

Globigerinoidesella fistulosa is a short-ranging morphospecies with a distinct stratigraphic range. Both its origination and extinction have been used as markers in Neogene planktonic foraminiferal biostratigraphy (Wade et al. 2011). *Globigerinoidesella fistulosa* evolved from the *Trilobatus sacculifer* plexus in the late Pliocene (King et al. 2020; Raffi et al. 2020) and went extinct in the early Pleistocene, marking the base of Subzone PT1a (Raffi et al. 2020). It is assigned to the genus *Globigerinoidesella* (El-Naggar 1971), as the radially elongated protuberances on the final chambers are considered a genus-level characteristic (Spezzaferri et al. 2015). The phylogenetic relationships are well constrained, and the morphospecies *T. sacculifer* and *G. fistulosa* are morphologically disparate (Poole and Wade 2019), but intermediate specimens bridge the morphological evolution (Fig. 2) and remain as common as *G. fistulosa* sensu stricto (s.s.) throughout the stratigraphic range of *G. fistulosa* (Poole and Wade 2019). *Trilobatus sacculifer* has a much longer stratigraphic range. It evolved in the early Miocene (Kennett and Srinivasan 1983) and persists throughout the stratigraphic range of *G. fistulosa*. It is still alive today, occupying the mixed layer (Rebotim et al. 2017) in warm tropical oceans and harboring some of the highest concentrations of algal photosymbionts in modern planktonic foraminifera (Kucera 2007; Takagi et al. 2019). Geochemical data indicate that *G. fistulosa* had the same habitat as members of the *T. sacculifer* plexus (Poole 2017).

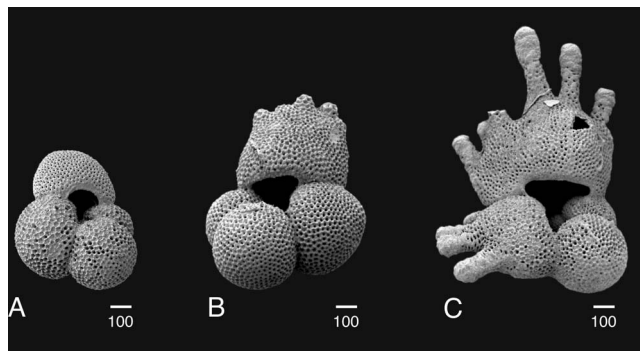


Figure 2. A, *Trilobatus sacculifer* (re-illustrated from Poole and Wade 2019: fig. 9D); B, an intermediate form between *T. sacculifer* and *Globigerinoidesella fistulosa* (re-illustrated from Poole and Wade 2019: fig. 11L); C, *G. fistulosa* (re-illustrated from Poole and Wade 2019: fig. 13J). All specimens from Ocean Drilling Program (ODP) Site 1115. Scale bars, 100 µm.

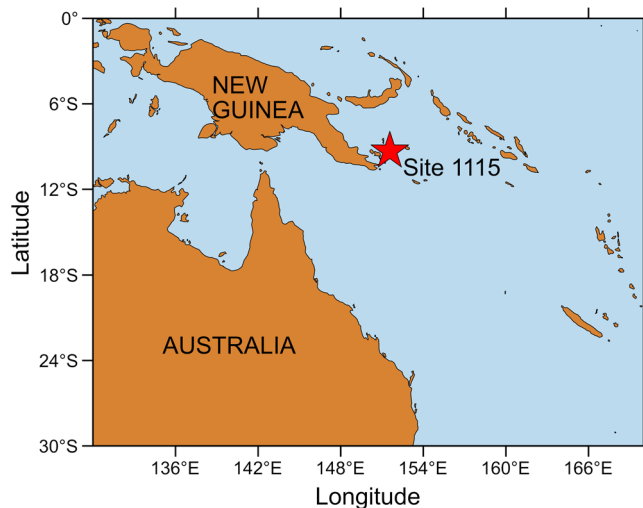


Figure 3. Location of Ocean Drilling Program (ODP) Site 1115 in the western Woodlark Basin, equatorial Pacific.

Materials

Ocean Drilling Program (ODP) Site 1115 is located in the western Woodlark Basin, western Pacific (9°11.382'S, 151°34.437'E) at a water depth of 1149 m; Shipboard Scientific Party 1999; Fig. 3). Hole 1115B was chosen primarily because the *G. fistulosa* specimens are abundant and well developed. The lowest occurrence of *G. fistulosa* is difficult to establish at Hole 1115B. The ancestor *T. sacculifer* occasionally grows incipient protuberances, which gradually gave rise to *G. fistulosa*. We follow Poole and Wade (2019) and limit *G. fistulosa* s.s. to specimens typically possessing four broad, flattened final chambers that increase rapidly in size, with one or more finger-like protuberances, multiple supplementary apertures, and a distinct lip on the primary aperture. Therefore, our lowest occurrence of *G. fistulosa* s.s. is higher than indicated for Hole 1115B by Shipboard Scientific Party (1999), who used an older, less-restricted taxonomic concept. Our sampling method was to examine end-members, that is, near the first occurrence of *G. fistulosa* s.s., and samples toward the end of the *G. fistulosa* range. To ensure maximum morphological differentiation with its ancestor, we analyzed 11 pre-

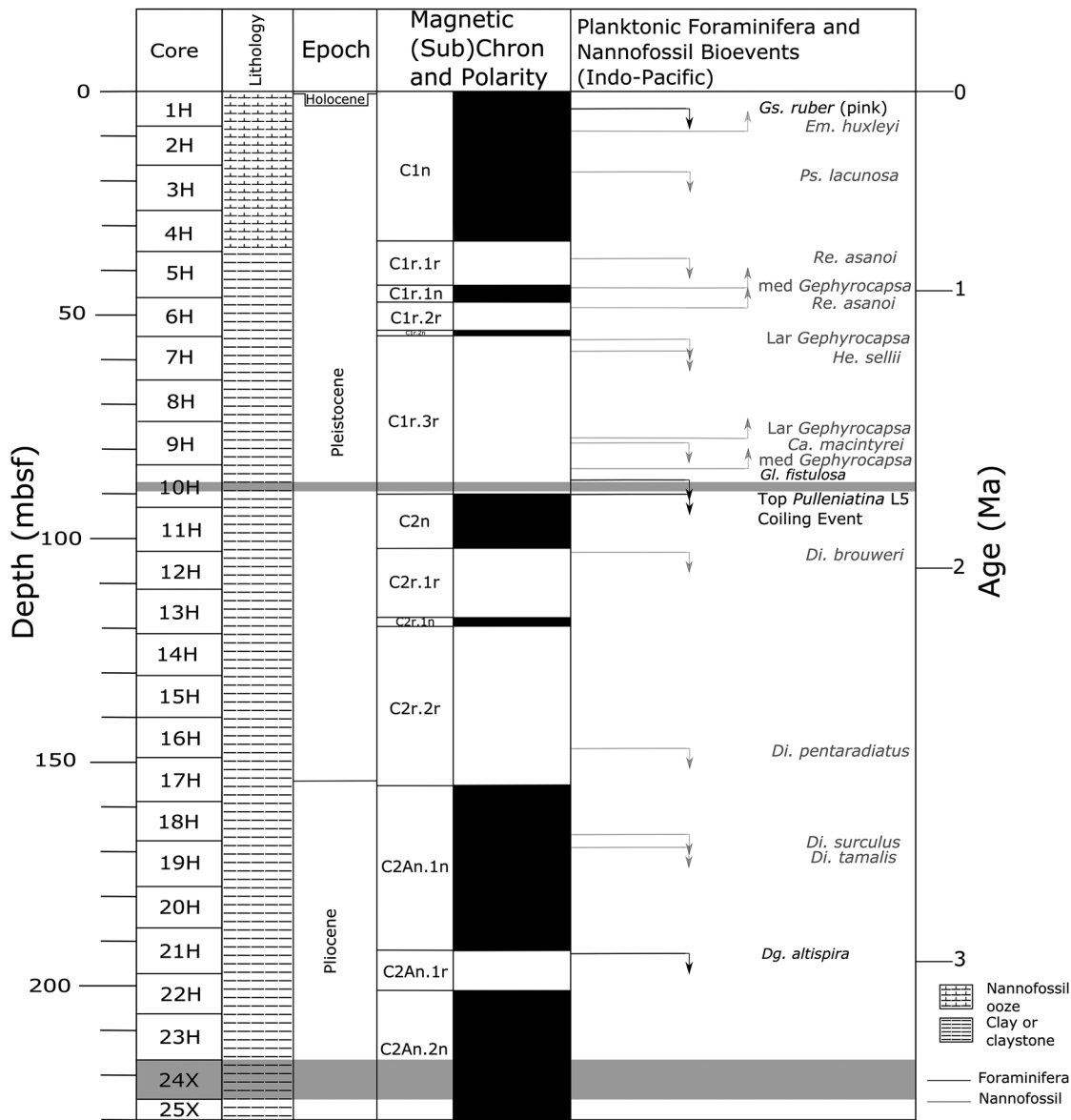


Figure 4. Magneto- and biostratigraphy at Ocean Drilling Program (ODP) Hole 1115B. Gray shaded boxes indicate intervals examined in this study for morphometric analysis. Paleomagnetic chrons and bioevents from Chuang et al. (2018), supplemented by calcareous nannofossil (right-aligned in gray) and planktonic foraminifera (left-aligned in black) biostratigraphy in Poole (2017).

speciation late Pliocene samples containing solely *T. sacculifer* plexus specimens (*Trilobatus trilobus*, *Trilobatus immaturus*, *Trilobatus sacculifer*, and *Trilobatus quadrilobatus*) from 24X (216.82–224.02 m below seafloor [m bsf]), and one time slice close to the top of the stratigraphic range of *G. fistulosa*, containing both *G. fistulosa* and contemporary specimens of the *T. sacculifer* plexus. Three closely spaced samples were analyzed from core 10H (mean depth: 88 m bsf), where *T. sacculifer*, *G. fistulosa*, and intermediate specimens are all present in each sample. Samples from 10H were pooled to increase the sample size and statistical power. Samples were dry sieved at the 250 μm size fraction to avoid inclusion of juvenile specimens. Adult specimens of both study species are much larger than 250 μm across, and there was no abrupt cutoff in the size data (see “Results” section and figures cited therein), so there was minimal risk of missing smaller adult specimens. All samples were picked for all *T. sacculifer* plexus and *G. fistulosa* tests, resulting in more than 900 specimens.

Specimens were positioned in umbilical view and imaged using a camera mounted on a light microscope. Images were analyzed using the Image Pro Premier software v. 9.3.

Stratigraphy

Chuang et al. (2018) provide an integrated stratigraphy for Site 1115, incorporating paleomagnetic reversal events with planktonic foraminifer and calcareous nannofossil bioevents and high-resolution oxygen isotope analysis tied to the benthic foraminifer oxygen isotope reference curve (LR04 stack; Lisiecki and Raymo 2005). Unfortunately, the Chuang et al. (2018) integrated stratigraphy ends slightly younger than the oldest part of our studied interval. We used biostratigraphy (Poole 2017; Chuang et al. 2018) and magnetostratigraphy (Takahashi et al. 2001) to determine the age of the samples studied, extrapolating back in time from the tuned record of Chuang et al. (2018) (Fig. 4, Table 1).

Chuang et al. (2018) used the magnetochronology of Cande and Kent (1995), and we have refrained from updating the Site 1115 record to more recently published magnetochronologies to keep our timescales consistent. Note, the biochronology of the bottom of the *Pulleniatina* L5 coiling shift in Chuang et al. (2018) is significantly older (~127 kyr) than calibrations from other Indo-Pacific sites (Pearson et al. 2023), thus we have not included this event in Figure 4. However, the astronomical calibration for top of the *Pulleniatina* L5 coiling shift at 1.777 ± 0.003 Ma is extremely consistent with the global calibration of 1.78 ± 0.01 Ma from multiple Indo-Pacific sites (Pearson et al. 2023). We find the highest occurrence of *G. fistulosa* between samples 10H-3 104–106 cm and 10H-3 95–97 cm (87.25 and 87.16 m bsf, respectively), giving a mean depth of 87.21 m bsf, which is a slightly higher level than in the Shipboard Scientific Party (1999) and Chuang et al. (2018), due to our higher-resolution sampling.

Analysis

All specimens were analyzed for total test area and curvature as measured from two-dimensional images (Fig. 5). Test curvature is calculated as follows:

$$C = \frac{P^2}{4\pi A} \quad (1)$$

Here P is test perimeter (μm) and A is test area (μm^2). The equation divides specimen perimeter length by surface area, as measured from the umbilical side. Lengthier perimeters score higher curvature values, and thus specimens that are lobate with high numbers of protuberances, such as *G. fistulosa* s.s., will have higher curvature values than specimens with a more rounded test periphery, such as *T. sacculifer* s.s.

We study allometric relationships between test size and curvature to detect the presence of heterochrony during speciation. Allometry can be expressed in the classic power-law equation of Huxley (1932):

$$y = bx^\alpha \quad (2)$$

Here, α and b are constants (α is the scaling exponent coefficient), x is area, and y is curvature. When expressed in logarithmic-transformed notation, the scaling relationship becomes linear:

$$\log y = \log b + \alpha \log x \quad (3)$$

Here, α is the slope of the relationship and $\log(b)$ is the intercept. Both determine the type of heterochrony quantitatively: unchanged slopes and intercepts indicate hyper- or hypomorphosis (Fig. 1A,D), whereas a change in intercept points to pre-/post-displacement (Fig. 1B,E) and a change in slope shows acceleration or deceleration (Fig. 1C,F).

Differences in slopes and intercepts among species and time slices were quantified with linear mixed-effect models using the R package nlme (v. 3.1.152; Pinheiro et al. 2021; R Core Team 2021). The models look for linear trends among subsets of the data (here: species or time slices) by comparing support for four different scenarios:

1. no overall trend between curvature and area with a consistent slope across species;
2. no overall trend between curvature and area, but varying species-specific slopes;
3. a relationship between curvature and area with a consistent slope across species; or
4. a relationship between curvature and area with species-specific slopes.

Variance differences among species or time slices were assessed using the *varIdent* function in nlme (Pinheiro and Bates 2000). The model with the lowest Akaike information criterion (AIC) value (a measure for model parsimony) and the highest Akaike weight (a measure for relative model likelihood) has the most statistical support among those models fit.

Results

In the oldest studied samples, preceding the appearance of *Globigerinoidesella fistulosa*, *Trilobatus sacculifer* alternates between intervals of low and high curvature, whereas average size remains unchanged (Fig. 6), resulting in parallel allometric slopes with different intercepts. The linear mixed-effect models confirm that the size–curvature slopes remain parallel throughout the pre-speciation interval (Table 2). After speciation, the intermediate specimens also show curves comparable to that of *T. sacculifer*, but with intermediate specimens showing both larger size and higher curvature than the ancestral forms (Fig. 7). *Globigerinoidesella fistulosa* is larger than both *T. sacculifer* and intermediate forms, although it should be noted that maximum size varies very little among species. Rather, the range in size of both *G. fistulosa* and intermediate specimens is narrower and concentrated at the larger end of the size range of *T. sacculifer* (Fig. 7). In contrast, the range of curvature values for *G. fistulosa* is much higher than for ancestral forms and increases strongly with size, resulting in an allometric slope significantly different from its ancestors (Fig. 7, Table 3). A visual inspection of the residuals shows that they are approximately normally distributed, satisfying the model prerequisites (see Figs. S1 and S2 available at <https://doi.org/10.5281/zenodo.14525398>).

Discussion

We study allometric relationships between test size and curvature to detect the presence of heterochrony during speciation. The allometric slopes in *Trilobatus sacculifer* immediately before the origination of *Globigerinoidesella fistulosa* show shifts between high and low curvature (Fig. 6). The parallel slopes, and similar size throughout the pre-speciation interval suggest a pattern of alternating pre- and post-displacement (Fig. 1B,E). Changes in *T. sacculifer* outline shape are primarily driven by variation in the shape of the saclike final chamber (Poole and Wade 2019), suggesting that in the pre-speciation interval, the *T. sacculifer* plexus alternated between more and less “*fistulosa*-like” final chambers. These phases could be a plastic response to local environmental change.

Our morphometric analyses reveal an alternating pattern of low and intermediate curvature in the *T. sacculifer* plexus (Fig. 6). This indicates that even before the origination of *G. fistulosa*, some of the morphological variation necessary to produce the new species was already present in the ancestor. However, pre-displacement was not enough to result in the unusual final morphology of *G. fistulosa*. The increase in average size of intermediate specimens compared with *T. sacculifer* (Fig. 7) points to hypermorphosis (Fig. 1A) on top of continued pre-displacement

Table 1. Sample ID, depth, and number of analyzed specimens (*n*) per sample. The pooled sample contains specimens from three pooled, closely spaced samples of 1115B-10H with an average depth of 88 m below seafloor (m bsf).

Morphospecies	Hole 1115B core sample	Depth (m bsf)	<i>n</i>
<i>Globigerinoidesella fistulosa</i>	Pooled sample	88	208
Intermediate	Pooled sample	88	56
<i>Trilobatus sacculifer</i>	Pooled sample	88	167
<i>T. sacculifer</i>	24X-01 51–53 cm	216.82	37
<i>T. sacculifer</i>	24X-01 100–102 cm	217.31	24
<i>T. sacculifer</i>	24X-02 50–52 cm	218.31	38
<i>T. sacculifer</i>	24X-02 100–102 cm	218.81	56
<i>T. sacculifer</i>	24X-03 41–43 cm	219.72	35
<i>T. sacculifer</i>	24X-03 98–100 cm	220.29	48
<i>T. sacculifer</i>	24X-04 41–43 cm	220.92	40
<i>T. sacculifer</i>	24X-04 100–102 cm	221.51	57
<i>T. sacculifer</i>	24X-05 50–52 cm	222.51	36
<i>T. sacculifer</i>	24X-05 100–102 cm	223.01	35
<i>T. sacculifer</i>	24X-06 51–53 cm	224.02	70

through higher curvature at similar sizes in intermediate specimens. The final transition from intermediate specimens to *G. fistulosa* is marked by a steeper allometric slope than those of both *T. sacculifer* and intermediate specimens (Fig. 7). Additionally, *G. fistulosa* often develops protuberances on multiple chambers in the final whorl (Poole and Wade 2019), which points to further pre-displacement by earlier onset of protuberances and likely contributes to the observed high curvature values. These results indicate that the origination of *G. fistulosa* involved a combination of two peramorphic expressions: pre-displacement through earlier onset of more pronounced protuberances and acceleration through a steeper allometric slope than its ancestor.

The steep allometric slope in *G. fistulosa* is likely directly related to the high number of protuberances in the species. The area of the protuberances is very small compared with the total test area, whereas a single protuberance can increase shell perimeter by as much as 50%. The underfitting of the slope at the highest curvature values is likely the result of a handful of specimens

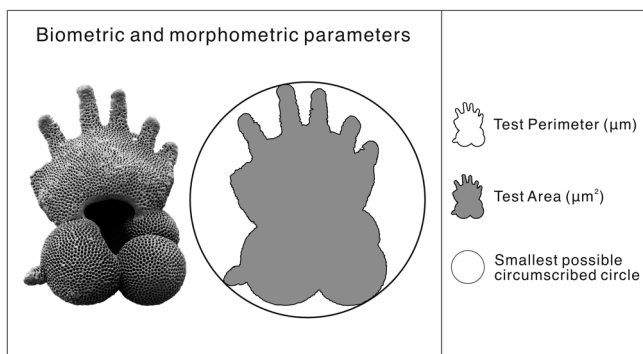


Figure 5. Biometric and morphometric parameters measured on *Trilobatus sacculifer* and *Globigerinoidesella fistulosa*.

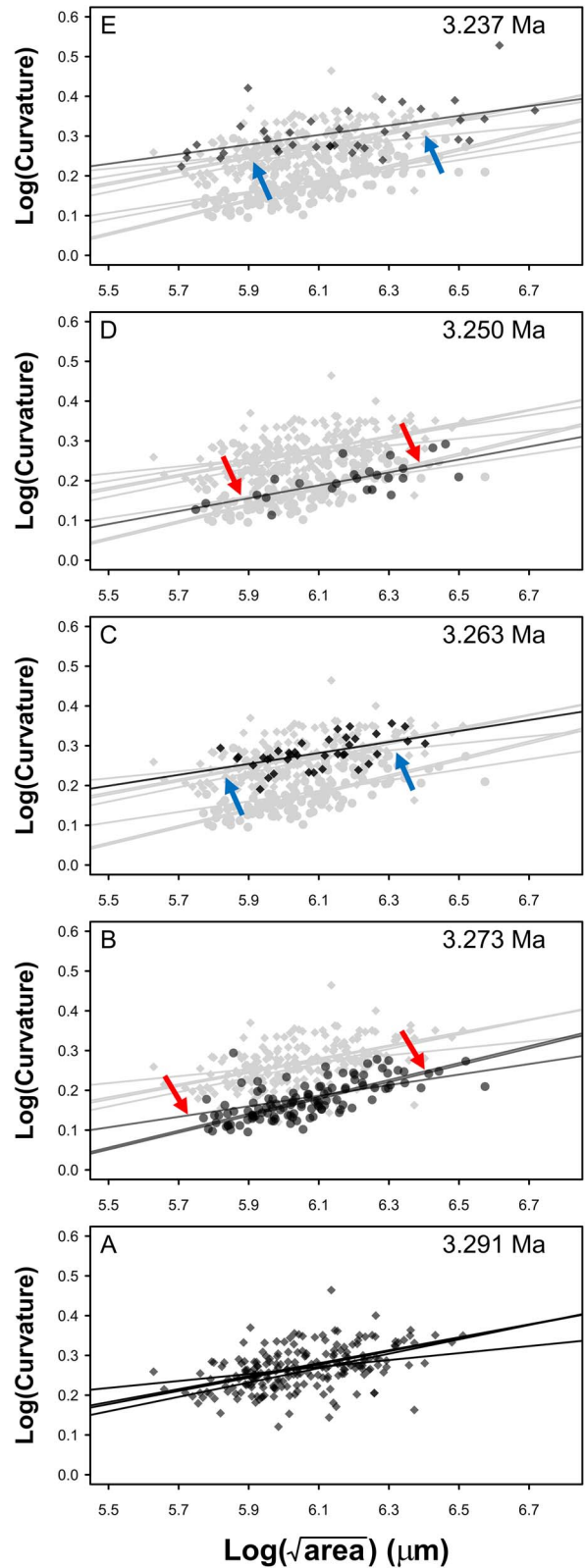


Figure 6. *Trilobatus sacculifer* size and shape allometry in five time intervals from oldest (A) to youngest (E) preceding the origination of *Globigerinoidesella fistulosa*. Black dots represent data from each panel's time interval, whereas gray dots show older data. Blue and red arrows indicate pre- and post-displacement, respectively. Most stages include several samples: stage (A) contains all samples from cores 24X-06 and 24X-05, stage (B) contains all samples from core 24X-04, stage (C) contains all samples from core 24X-03, stage (D) contains all samples from core 24X-02, and stage (E) contains all samples from core 24X-01. See Table 1 for full sample IDs.

Table 2. Log likelihood, Akaike information criterion (AIC), and Akaike weights for all four analyzed models of *Trilobatus sacculifer* area and curvature preceding origination of *Globigerinoidesella fistulosa*. Δ AIC represents the difference between AIC and the set's minimum AIC. The best-performing model based on AIC and Akaike weight is indicated in bold.

Model	Log likelihood	Degrees of freedom	AIC	Δ AIC	Akaike weight	Marginal R^2	Conditional R^2
m0: Curve $\sim 1 + (1 \mid \text{species})$	756.9	13	-1487.8	188.6	0.000	0.000	0.390
m1: Curve $\sim 1 + (\text{curve} \mid \text{species})$	831.9	15	-1633.7	42.8	0.000	0.000	0.590
m2: Curve $\sim \text{area} + (1 \mid \text{species})$	852.2	14	-1676.5	0.0	0.711	0.140	0.543
m3: Curve $\sim \text{area} + (\text{area} \mid \text{species})$	853.3	16	-1674.7	1.8	0.289	0.142	0.552

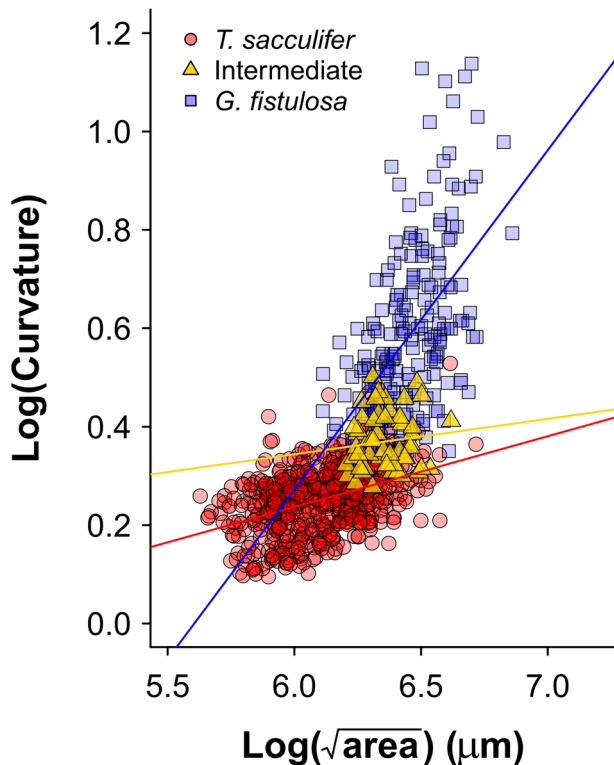


Figure 7. Log size and curvature for *Trilobatus sacculifer*, intermediate, and *Globigerinoidesella fistulosa* specimens. Straight lines show linear regressions for each species (*T. sacculifer*: $R^2 = 0.17$, $p < 0.001$; intermediate: $R^2 = 0.014$, $p < 0.001$; *G. fistulosa*: $R^2 = 0.29$, $p < 0.001$).

with multiple long protuberances that disproportionately affect the curvature values.

There are numerous described cases of heterochrony in the Cenozoic fossil record of planktonic foraminifera, and both paedomorphic and peramorphic expressions have been observed in quantitative and qualitative studies. For example, studies of the

Paleocene–Eocene *Globanomalina chapmani*–*Globanomalina luxorensis*–*Pseudohastigerina wilcoxensis* lineage found evidence of hypermorphosis or acceleration (Berggren *et al.* 1967) and pre-displacement (Speijer and Samir 1997). The Eocene transition from *Globanomalina australiformis* to *Turborotalia frontosa* is interpreted as resulting from hypermorphosis (Olsson and Hemleben 2006; Pearson *et al.* 2006b). Interestingly, the subsequent *Turborotalia* lineage demonstrates a regressive paedomorphic trend that effectively reversed the former hypermorphosis expression (Pearson *et al.* 2006b). Wei (1994) conducted a comprehensive study to calculate allometric “trajectories” for assessing heterochronic modes over time in morphological evolution within species of the *Globoconella puncticulata*–*Globoconella inflata* plexus. Following the divergence of *G. puncticulata* and *G. inflata*, both morphospecies underwent different modes of heterochrony (Wei 1994). In *G. puncticulata*, the change in allometric trajectories suggested acceleration, with later forms developing higher peripheral roundness in comparison to same-sized ancestral forms (Wei 1994). In *G. inflata*, the initial post-displacement trend is interpreted as a delay in the onset of the neanic ontogenetic stage and a probable cause of divergence between the morphospecies (Wei 1994). Interestingly, this is followed by a reversing trend of pre-displacement (Wei 1994). Finally, Morard *et al.* (2019) combined genetics and morphological measurements in modern species of the *Globigerinoides* genus to explain the apparent mismatch between morphological disparity and a high degree of genetic kinship. They found that relatively large morphological differences between closely related species can be attained by small changes in the developmental sequence, highlighting the importance of considering heterochronic expressions when studying planktonic foraminifera evolution.

The peramorphic expressions of both pre-displacement and acceleration in the origination of *G. fistulosa* bears close resemblance to the evolution of Eocene *Hantkenina*. Hantkeninids are bizarre-looking planktonic foraminifera characterized by tubulospines. The tubulospines first developed on the final, adult chambers, before earlier trait onset in later hantkeninid species (Pearson and Coxall 2014). Such a shift to earlier trait

Table 3. Log likelihood, Akaike information criterion (AIC), and Akaike weights for all four analyzed models comparing *Trilobatus sacculifer*, *Globigerinoidesella fistulosa*, and intermediate specimens' area and curvature. Δ AIC represents the difference between AIC and the set's minimum AIC. The best-performing model based on AIC and Akaike weight is indicated in bold.

Model	Log likelihood	Degrees of freedom	AIC	Δ AIC	Akaike weight	Marginal R^2	Conditional R^2
m0: Curve $\sim 1 + (1 \mid \text{species})$	1006.0	5	-2001.9	179.1	0.000	0.000	0.473
m1: Curve $\sim 1 + (\text{curve} \mid \text{species})$	1097.5	7	-2181.0	0.0	0.781	0.000	0.510
m2: Curve $\sim \text{area} + (1 \mid \text{species})$	1076.4	6	-2140.7	40.3	0.000	0.024	0.440
m3: Curve $\sim \text{area} + (\text{area} \mid \text{species})$	1097.3	8	-2178.5	2.5	0.219	0.013	0.500

(tubulospine) development in later morphospecies, such as *Hantkenina mexicana*, may therefore indicate pre-displacement, although the later morphospecies are generally also larger than the transitional forms, pointing to hypermorphosis (Pearson and Coxall 2014). To our knowledge, the hantkeninids and *G. fistulosa* are the only species of planktonic foraminifera whose origination included multiple expressions of heterochrony. Possibly, their extreme shapes could only be formed through multiple developmental shifts, which might explain why unusual shapes such as protuberances and tubulospines are so rare in planktonic foraminifera.

In terms of mechanisms, although the aforementioned heterochronic changes explain how *G. fistulosa* managed to reach a more extreme shape than most other planktonic foraminifera, the drivers of these morphological adaptations are harder to interpret. Schmidt et al. (2016) showed that *T. sacculifer* size and shape are partly controlled by temperature. The *G. fistulosa* stratigraphic range includes the onset of the Northern Hemisphere glaciation (~3.5 to 2.5 Ma) (Bailey et al. 2013; Westerhold et al. 2020). During this interval, Earth transitioned from a unipolar glacial state, with large ice sheets only on Antarctica, to one that was sufficiently cool by ~2.7 Ma to induce growth of large ice sheets in the Northern Hemisphere and associated rafting of icebergs across the subpolar North Atlantic Ocean (Shackleton et al. 1984). The high-resolution oxygen isotope record of *T. sacculifer* at Site 1115 does not indicate any dramatic change associated with the extinction of *G. fistulosa* (Chuang et al. 2018). Furthermore, *G. fistulosa* was restricted to the tropical oceans, and its exposure to environmental change originating in the high northern latitudes was therefore likely limited.

Both the *T. sacculifer* plexus and *G. fistulosa* are spinose, occupy the mixed layer, and harbor algal photosymbionts. It has been shown that the acquisition of symbionts is necessary for *T. sacculifer* to achieve maximum sizes (Bé et al. 1982). The large size of *G. fistulosa* compared with *T. sacculifer* would have required even more symbionts than *T. sacculifer*, but the surface area to volume ratio in globular chambers of planktonic foraminifera, and thus space for symbionts, decreases with increasing volume. The protuberances in *G. fistulosa* potentially counteract this trend by increasing surface area to host more symbionts. Modern species with shells that have a high surface area to volume ratio often show a greater rise in photosymbionts with increasing size than more spherical ones (Takagi et al. 2019), suggesting that irregular shapes are beneficial to symbiont activity. This hypothesis could be tested in future studies by comparing stable carbon isotope trends between *G. fistulosa* and *T. sacculifer* to test for differences in symbiont activity. The protuberances themselves are spinose (Poole and Wade 2019), further increasing effective test size. Other digitate species such as the hantkeninids have been argued to evolve elongated chambers to increase effective test size and food-gathering efficiency (Coxall et al. 2007), a mechanism that possibly further helped *G. fistulosa* to reach and maintain a large body size. Finally, it should be noted that there might not be any clear evolutionary advantage of the protuberances. Much of the functional morphology of foraminiferal shell shape remains unclear (Renaud and Schmidt 2003; Caromel et al. 2014), and the development of some morphological features may not have a specific functional response. An evolutionary advantage or fulfillment of a particular function does not need to be assumed by the development of a trait, such as protuberances in *G. fistulosa*.

Conclusions

The origination of the unusual test size and shape of *Globigerinoidesella fistulosa* was the result of a combination of pre-displacement and acceleration of ancestral traits found in *Trilobatus sacculifer*. These results imply that shifts in multiple developmental expressions are required for the origination of unusual morphologies. As both ancestor and descendant species continued to thrive following the origination of *G. fistulosa*, the drivers of morphological change are unlikely to be environmental variations that favored one species over the other. Our work provides a case study of the complex developmental changes required to produce ornate shell shapes and highlights the importance of development in the origination of unusual forms.

Acknowledgments. We are grateful to R. Morard, M. R. Petruzzo, and an anonymous reviewer whose comments significantly improved the article. Thanks to Z. Tian, N. Staikidou, and D. King for assistance with figures. This study was funded through a UK Natural Environment Research Council (NERC) studentship to C.R.P. and NERC grant NE/P019013/1 to B.S.W. A.B. and T.H.G.E. were funded through NERC grant NE/P019269/1. Samples were provided by the International Ocean Discovery Program (IODP), which is sponsored by the U.S. National Science Foundation and participating countries.

Competing Interest. The authors declare no competing interests.

Data Availability Statement. Data are available from the Dryad repository: <https://doi.org/10.5061/dryad.3bk3j9kqh>.

Literature Cited

- Alberch, P., S. J. Gould, G. F. Oster, and D. B. Wake. 1979. Size and shape in ontogeny and phylogeny. *Paleobiology* 5:296–317.
- Aze, T., T. H. Ezard, A. Purvis, H. K. Coxall, D. R. Stewart, B. S. Wade, and P. N. Pearson. 2011. A phylogeny of Cenozoic macroperforate planktonic foraminifera from fossil data. *Biological Reviews of the Cambridge Philosophical Society* 86:900–927.
- Bailey, I., G. M. Hole, G. L. Foster, P. A. Wilson, C. D. Storey, C. N. Trueman, and M. E. Raymo. 2013. An alternative suggestion for the Pliocene onset of major Northern Hemisphere glaciation based on the geochemical provenance of North Atlantic Ocean ice-rafted debris. *Quaternary Science Reviews* 75:181–194.
- Bé, A. W. H., H. J. Spero, and O. R. Anderson. 1982. Effects of symbiont elimination and reinfection on the life processes of the planktonic foraminifer *Globigerinoides sacculifer*. *Marine Biology* 70:73–86.
- Berggren, W. A., R. K. Olsson, and R. A. Reymont. 1967. Origin and development of the foraminiferal genus *Pseudohastigerina* Banner and Blow, 1959. *Micropaleontology* 13:265–288.
- Brummer, G.-J. A., C. Hemleben, and M. Spindler. 1986. Planktonic foraminiferal ontogeny and new perspectives for micropaleontology. *Nature* 319:50–52.
- Brummer, G.-J. A., C. Hemleben, and M. Spindler. 1987. Ontogeny of extant spinose planktonic foraminifera (*Globigerinidae*): a concept exemplified by *Globigerinoides sacculifer* (Brady) and *G. ruber* (d'Orbigny). *Marine Micropaleontology* 12:357–381.
- Cande, S. C., and D. V. Kent. 1995. Revised calibration of the geomagnetic polarity timescale for the Late Cretaceous and Cenozoic. *Journal of Geophysical Research: Solid Earth* 100(B4):6093–6095.
- Caromel, A. G. M., D. N. Schmidt, J. C. Phillips, and E. J. Rayfield. 2014. Hydrodynamic constraints on the evolution and ecology of planktic foraminifera. *Marine Micropaleontology* 106:69–78.
- Caromel, A. G., D. N. Schmidt, I. Fletcher, and E. J. Rayfield. 2016. Morphological change during the ontogeny of the planktic foraminifera. *Journal of Micropaleontology* 35:2–19.
- Caromel, A. G. M., D. N. Schmidt, and E. J. Rayfield. 2017. Ontogenetic constraints on foraminiferal test construction. *Evolution and Development* 19:157–168.

- Chaisson, W. P., and M. R. Leckie. 1993. High-resolution Neogene planktonic foraminifer biostratigraphy of Site 806, Ontong Java Plateau (western equatorial Pacific). *Proceedings of the Ocean Drilling Program, Scientific Results* 130:137–178.
- Chen, W.-L., J.-C. Kang, K. Kimoto, Y.-F. Song, G.-C. Yin, R. E. Swisher, C.-H. Lu, L.-W. Kuo, J.-J. S. Huang, and L. Lo. 2023. μ -Computed tomographic data of fossil planktonic foraminifera from the western Pacific Ocean: a dataset concerning two biostratigraphic events during the Early Pleistocene. *Frontiers in Ecology and Evolution* 11:1–7.
- Chuang, C.-K., L. Lo, C. Zeeden, Y.-M. Chou, K.-Y. Wei, C.-C. Shen, H.-S. Mii, Y.-P. Chang, and Y.-H. Tung. 2018. Integrated stratigraphy of ODP Site 1115 (Solomon Sea, southwestern equatorial Pacific) over the past 3.2 Ma. *Marine Micropaleontology* 144:25–37.
- Coxall, H. K., P. A. Wilson, P. N. Pearson, and P. F. Sexton. 2007. Iterative evolution of digitate planktonic foraminifera. *Paleobiology* 33:495–516.
- Dobrev, M. P., J. Camacho, and A. Abzhanov. 2022. Time to synchronize our clocks: connecting developmental mechanisms and evolutionary consequences of heterochrony. *Journal of Experimental Zoology B* 338:87–106.
- El-Naggar, Z. R. 1971. On the classification, evolution and stratigraphical distribution of the Globigerinacea. *Proceedings of the II Planktonic Conference* 1971:421–476.
- Falcon-Lang, H. J. 2015. A calamitalean forest preserved in growth position in the Pennsylvanian coal measures of South Wales: implications for palaeoecology, ontogeny and taphonomy. *Review of Palaeobotany and Palynology* 214:51–67.
- Gould, S. J. 1977. *Ontogeny and phylogeny*. Harvard University Press, Cambridge, Mass.
- Huxley, J. 1932. *Problems of relative growth*. Methuen, London.
- Jones, D. S., and S. J. Gould. 1999. Direct measurement of age in fossil *Gryphaea*: the solution to a classic problem in heterochrony. *Paleobiology* 25:158–187.
- Kennett, J. P., and M. S. Srinivasan. 1983. *Neogene planktonic foraminifera. A phylogenetic atlas*. Hutchinson Ross Publishing, Stroudsburg, Pa.
- Keyte, A. L., and K. K. Smith. 2014. Heterochrony and developmental timing mechanisms: changing ontogenies in evolution. *Seminars in Cell and Developmental Biology* 34:99–107.
- King, D. J., B. S. Wade, R. D. Liska, and C. G. Miller. 2020. A review of the importance of the Caribbean region in Oligo-Miocene low latitude planktonic foraminiferal biostratigraphy and the implications for modern biogeochronological schemes. *Earth-Science Reviews* 202:1–27.
- Kucera, M. 2007. Planktonic foraminifera as tracers of past oceanic environments. Pp. 213–262 in A. De Vernal, ed. *Proxies in Late Cenozoic paleoceanography*. Elsevier, Amsterdam.
- Lazarus, D. B. 2011. The deep-sea microfossil record of macroevolutionary change in plankton and its study. In A. J. McGowan, and A. B. Smith, eds. *Comparing the geological and fossil records: implications for biodiversity studies*. Geological Society of London Special Publication 358:141–166.
- Lisiecki, L. E., and M. E. Raymo. 2005. A Pliocene–Pleistocene stack of 57 globally distributed benthic $\delta^{18}\text{O}$ records. *Paleoceanography* 20:1–17.
- McKinney, M. L. 1986. Ecological causation of heterochrony: a test and implications for evolutionary theory. *Paleobiology* 12:282–289.
- McKinney, M., and K. McNamara. 1991. *Heterochrony: the evolution of ontogeny*. Plenum, New York.
- McNamara, K. J. 1986. A guide to the nomenclature of heterochrony. *Journal of Paleontology* 60:4–13.
- McNamara, K. J. 2012. Heterochrony: the evolution of development. *Evolution: Education and Outreach* 5:203–218.
- Morard, R., A. Füllberg, G. A. Brummer, M. Greco, L. Jonkers, A. Wizemann, A. K. M. Weiner, *et al.* 2019. Genetic and morphological divergence in the warm-water planktonic foraminifera genus *Globigerinoides*. *PLoS ONE* 14:e0225246.
- Norris, R. D. 1991. Biased extinction and evolutionary trends. *Paleobiology* 17:388–399.
- Norris, R. D. 2000. Pelagic species diversity, biogeography, and evolution. *Paleobiology* 26:236–258.
- Olsson, R. K., and C. Hemleben. 2006. Taxonomy, biostratigraphy, and phylogeny of Eocene *Globanomalina*, *Planoglobanomalina* n. gen and *Pseudohastigerina*. Pp. 257–326 in P. N. Pearson, R. K. Olsson, B. T. Huber, C. Hemleben, and W. A. Berggren, eds. *Atlas of Eocene planktonic foraminifera*. Cushman Foundation Special Publications. GeoScienceWorld, McLean, Va.
- Olsson, R. K., C. Hemleben, W. A. Berggren, and B. T. Huber, eds. 1999. *Atlas of Paleocene planktonic foraminifera*. Smithsonian Contributions to Paleobiology 85. Smithsonian Institution Press, Washington, D.C.
- Parker, F. L. 1967. Late Tertiary biostratigraphy (planktonic foraminifera) of tropical Indo-Pacific deep-sea cores. *Bulletin of American Paleontology* 52:115–203.
- Pearson, P. N., and H. K. Coxall. 2014. Origin of the Eocene planktonic foraminifer *Hantkenina* by gradual evolution. *Palaeontology* 57:243–267.
- Pearson, P. N., R. K. Olsson, B. T. Huber, C. Hemleben, and W. A. Berggren, eds. 2006a. *Atlas of Eocene planktonic foraminifera*. Cushman Foundation Special Publications. GeoScienceWorld, McLean, Va.
- Pearson, P. N., V. Premec-Fucek, and I. Premoli Silva. 2006b. Taxonomy, biostratigraphy, and phylogeny of Eocene *Turborotalia*. Pp. 433–460 in P. N. Pearson, R. K. Olsson, B. T. Huber, C. Hemleben, and W. A. Berggren, eds. *Atlas of Eocene planktonic foraminifera*. Cushman Foundation Special Publications. GeoScienceWorld, McLean, Va.
- Pearson, P. N., J. Young, D. J. King, and B. S. Wade. 2023. Biochronology and evolution of *Pulleniatina* (planktonic foraminifera). *Journal of Micropaleontology* 42(2):211–255.
- Pinheiro, J., and D. Bates. 2000. Linear mixed-effect models: basic concepts and examples. In *Mixed-effect models in S and S-Plus*. Springer-Verlag, New York, pp. 3–56.
- Pinheiro, J., D. Bates, S. DebRoy, D. Sarkar, and R. C. Team. 2021. nlme: linear and nonlinear mixed effects models, R package version 3.1.152. CRAN. <https://svn.r-project.org/R-packages/trunk/nlme/> (Last accessed 2 August 2023).
- Poole, C. R. 2017. *The late Neogene planktonic foraminifera genus Globigerinoidesella: taxonomy, biostratigraphy, evolution and palaeoecology*. PhD thesis. University College London, London.
- Poole, C. R., and B. S. Wade. 2019. Systematic taxonomy of the *Trilobatus sacculifer* plexus and descendant *Globigerinoidesella fistulosa* (planktonic foraminifera). *Journal of Systematic Palaeontology* 17:1989–2030.
- Raffi, I., B. S. Wade, and H. Pälke. 2020. The Neogene Period. Pp. 1141–1215 in F. Gradstein, J. G. Ogg, M. D. Schmitz, and G. Ogg, eds. *Geologic time scale 2020*. Elsevier, Amsterdam.
- R Core Team. 2021. *R: a language and environment for statistical computing*. R Foundation for Statistical Computing, Vienna, Austria.
- Rebotim, A., A. H. L. Voelker, L. Jonkers, J. J. Waniek, H. Meggers, R. Schiebel, I. Fraile, M. Schulz, and M. Kucera. 2017. Factors controlling the depth habitat of planktonic foraminifera in the subtropical eastern North Atlantic. *Biogeosciences* 14:827–859.
- Reilly, S. M., E. Wiley, and D. J. Meinhardt. 1997. An integrative approach to heterochrony: the distinction between interspecific and intraspecific phenomena. *Biological Journal of the Linnean Society* 60:119–143.
- Renaud, S., and D. N. Schmidt. 2003. Habitat tracking as a response of the planktic foraminifer *Globorotalia truncatulinoides* to environmental fluctuations during the last 140 kyr. *Marine Micropaleontology* 49:97–122.
- Sanchez, S., A. de Ricqlès, R. Schoch, and J. S. Steyer. 2010. Developmental plasticity of limb bone microstructural organization in Apateton: histological evidence of paedomorphic conditions in branchiosaurs. *Evolution and Development* 12:315–328.
- Sander, P. M., and N. Klein. 2005. Developmental plasticity in the life history of a prosauropod dinosaur. *Science* 310:1800–1802.
- Schmidt, D. N., E. J. Rayfield, A. Cocking, and F. Marone. 2013. Linking evolution and development: synchrotron radiation X-ray tomographic microscopy of planktic foraminifers. *Palaeontology* 56:741–749.
- Schmidt, D. N., A. Caromel, O. Seki, J. W. B. Rae, and S. Renaud. 2016. Morphological response of planktic foraminifers to habitat modifications associated with the emergence of the Isthmus of Panama. *Marine Micropaleontology* 128:28–38.
- Shackleton, N. J., J. Backman, H. Zimmerman, D. V. Kent, M. A. Hall, D. G. Roberts, D. Schnitker, *et al.* 1984. Oxygen isotope calibration of the onset of ice-rafting and history of glaciation in the North Atlantic region. *Nature* 307:620–623.
- Shipboard Scientific Party. 1999. Site 1115. *Proceedings of the Ocean Drilling Program, Initial Reports* 180:1–226.

- Speijer, R. P., and A. M. Samir. 1997. *Globanomalina luxorensis*, a Tethyan biostratigraphic marker of latest Paleocene global events. *Micropaleontology* 43:51–62.
- Spezzaferri, S., M. Kucera, P. N. Pearson, B. S. Wade, S. Rappo, C. R. Poole, R. Morard, and C. Stalder. 2015. Fossil and genetic evidence for the polyphyletic nature of the planktonic foraminifera “*Globigerinoides*”, and description of the new genus *Trilobatus*. *PLoS ONE* 10:e0128108.
- Takagi, H., K. Kimoto, T. Fujiki, H. Saito, C. Schmidt, M. Kucera, and K. Moriya. 2019. Characterizing photosymbiosis in modern planktonic foraminifera. *Biogeosciences* 16:3377–3396.
- Takahashi, K., G. Cortese, G. M. Frost, S. Gerbaudo, A. M. Goodliffe, N. Ishikawa, K. S. Lackschewitz, et al. 2001. Summary of revised age assignment for ODP leg 180. In P. Huchon, B. Taylor, and A. Klaus, eds. *Proceedings of the Ocean Drilling Program, Scientific Results*. http://www.odp.tamu.edu/publications/180_SR/152/152.htm.
- Trueman, C. N., M. T. Chung, and D. Shores. 2016. Ecogeochemistry potential in deep time biodiversity illustrated using a modern deep-water case study. *Philosophical Transactions of the Royal Society B* 371:1–10.
- Wade, B. S., P. N. Pearson, W. A. Berggren, and H. Pälike. 2011. Review and revision of Cenozoic tropical planktonic foraminiferal biostratigraphy and calibration to the geomagnetic polarity and astronomical time scale. *Earth-Science Reviews* 104:111–142.
- Wade, B. S., R. K. Olsson, P. N. Pearson, B. T. Huber, and W. A. Berggren, eds. 2018. *Atlas of Oligocene planktonic foraminifera*. Cushman Foundation Special Publication 46. GeoScienceWorld, McLean, Va. 528 pp.
- Wei, K.-Y. 1994. Allometric heterochrony in the Pliocene–Pleistocene planktic foraminiferal clade *Globoconella*. *Paleobiology* 20:66–84.
- Wei, K.-Y., Z.-W. Zhang, and C. Wray. 1992. Shell ontogeny of *Globorotalia inflata*; I, growth dynamics and ontogenetic stages. *Journal of Foraminiferal Research* 22:318–327.
- Westerhold, T., N. Marwan, A. J. Drury, D. Liebrand, C. Agnini, E. Anagnostou, J. S. K. Barnet, et al. 2020. An astronomically dated record of Earth’s climate and its predictability over the last 66 million years. *Science* 369:1383–1387.
- Whittington, H. B. 1957. The ontogeny of trilobites. *Biological Reviews* 32:421–467.